A ''Self-Pinning'' Adhesive Based on Responsive Surface Wrinkles

Edwin P. Chan,[1]* Jeffrey M. Karp,[1,2,3] Robert S. Langer[1,4]

[1]Harvard-MIT Division of Health Sciences and Technology, Massachusetts Institute of Technology, Cambridge, Massachusetts 02139

[2]Center for Regenerative Therapeutics, Department of Medicine, Brigham and Women's Hospital, Harvard Medical School, Cambridge, Massachusetts 02319

[3]Harvard Stem Cell Institute, Harvard University, Cambridge, Massachusetts 02138

[4]Department of Chemical Engineering, Massachusetts Institute of Technology, Cambridge, Massachusetts 02139

Correspondence to: E. Chan (E-mail: edwin.chan@nist.gov) or J. M. Karp (E-mail: jkarp@rics.bwh.harvard.edu) or R. Langer (E-mail: rlanger@mit.edu)

Received 5 August 2010; revised 26 August 2010; accepted 15 September 2010; published online 22 October 2010
DOI: 10.1002/polb.22165

ABSTRACT: Surface wrinkles are interesting since they form spontaneously into well-defined patterns. The mechanism of formation is well-studied and is associated with the development of a critical compressive stress that induces the elastic instability. In this work, we demonstrate surface wrinkles that dynamically change in response to a stimulus can improve interfacial adhesion with a hydrogel surface through the dynamic evolution of the wrinkle morphology. We observe that this control is related to the local pinning of the crack separation pathway facilitated by the surface wrinkles during debonding, which is dependent on the contact time with the hydrogel. © 2010 Wiley Periodicals, Inc. J Polym Sci Part B: Polym Phys 49: 40–44, 2011

KEYWORDS: adhesion; adhesives; biomaterials; hydrogels; stimuli-sensitive polymers; surfaces; swelling

INTRODUCTION Interests in stimuli-responsive materials stem from their amazing ability to develop sudden macroscopic property changes in response to an external stimulus.[1] These materials are potentially useful in many applications that require the dynamic control of interfacial properties, such as adhesion,[2,3] friction,[4] and wettability.[5,6] One interesting concept involves utilizing surface wrinkles as stimuli-responsive materials. Surface wrinkles are a class of elastic instability that develops in response to a critical compressive stress.[3,6–14] Because the resultant topographic wrinkle patterns are well-defined, several groups have utilized stable surface wrinkles to tune the adhesion of "dry" polymer interfaces. The results are very interesting since soft polymer adhesion can be enhanced or suppressed, and this control is related to the surface wrinkles feature size-scale in relationship to a materials-defined length-scale. More recently, Hayward and coworkers have studied the dynamic response of wrinkled hydrogel materials.[7,15] The key result of their work is the demonstration of the dynamic change of the surface wrinkles via an external stimulus such as pH.

Based on these inspirations, we present a new strategy to tailor soft polymer adhesion via responsive surface wrinkles that takes advantage of a polymer's natural propensity to swell in a solvent as a stimulus to drive wrinkle formation. Specifically, we develop a Responsive Surface-wrinkled Adhesive (RSA) that changes wrinkle morphology as it swells in water. By interfacing this RSA material with a gelatin-based hydrogel, we show that interfacial adhesion can be controlled with contact time to the hydrogel surface. We illustrate that the primary mechanism of adhesion is associated with the topographical evolution of the wrinkled surface with contact time, which locally pins the crack propagation pathway as the RSA releases from the hydrogel. This approach is interesting as it takes advantage of a dynamic topographic surface to control adhesion.

EXPERIMENTAL

Materials

RSA films and probes were synthesized via photopolymerization by using a formulation of 74 wt % polyethylene glycol methyl ether acrylate, 24 wt % acrylic acid, and 2 wt % polyethylene glycol dimethacrylate (Sigma-Aldrich, St. Louis, MO), and 1 wt % Irgacure^{TM} 819 photoinitator (Ciba Specialty Chemicals, Tarrytown, NY). To fabricate the RSA hemispheres, the solution was deposited into a crosslinked dimethyl siloxane hemispherical mold and then covered with a glass substrate. The sample was then irradiated with UV ($\lambda = 365$ nm, intensity $= 20$ mW/cm^2) for 4 min, demolded

**Present address:* Polymers Division, National Institute of Standards and Technology, 100 Bureau Drive, Gaithersburg, Maryland 20899.

and then used without additional processing. Gelatin was used as the hydrogel material. The gelatin films were fabricated by mixing 12.5 wt % Bloom 225 (Sigma-Aldrich, St. Louis, MO) with 81.5 wt % hot deionized water. A 1 mL solution was deposited onto 2.54 cm^2 glass substrates and used immediately to minimize drying of the films.

Optical Profilometry

The wrinkle amplitude at the maximum wavelength was determined using a Zygo NewVIEW 6000 3D optical interferometer (Mirau 50X objective, Zygo Corporation, Middlefield, CT). Due to the difficulty in measuring the amplitude through a water medium, we measured the long time (at 10 min. swelling) amplitude by removing the excess water on the wrinkled surface and immediately measuring the amplitude.

Contact Adhesion Testing

Contact adhesion testing was used to measure the adhesion between the RSA and gelatin interface. Briefly, the test involves forming an interface between the RSA and gelatin, followed by subsequent separation of the interface. The test begins by bringing the RSA probe, with a 5 mm radius of curvature, into contact with the gelatin surface at a fixed displacement rate of 1.5 μm/s. After reaching the maximum compressive load of 2 mN, the probe is retracted from the gelatin to separate the interface at the same displacement rate. For the contact time studies, the probe was compressed at this load for the defined contact time. Then, the probe was retracted to cause separation at the same displacement rate. The contact times investigated were 0, 60, 120, 300, and 600 s. The load is monitored by a force transducer (Honeywell Sensotec, Columbus, OH) while the displacement is controlled by a nanopositioner (Burleigh Instruments IW-820, Exfo Burleigh Products Group, Victor, NY). The contact areas were recorded by an inverted optical microscope (2.5X objective, Nikon Instruments, Melville, NY). All the data were recorded via a custom-developed National Instruments LabVIEW® software.

RESULTS

Figure 1 demonstrates the dynamic change of the RSA when exposed to water. Within 5 sec of water exposure, the surface of the initially smooth RSA respond immediately by developing well-defined surface wrinkles [Fig. 1(a)]. These patterns are stable, as long as the surface remains hydrated, and persist over the entire swelling period. Additionally, the wavelength evolves with swelling time [Fig. 1(a,b)], with an initial wavelength of ~80 μm and a final value of ~540 μm. The wavelength measurements were determined by averaging the center-to-center distance between two adjacent wrinkles from the optical micrographs for five wrinkles to determine an average value. From optical profilometry, the amplitude is ~42 μm when the wavelength reaches its upper value. Beyond 5 min, the wavelength stabilizes to this upper value [Fig. 1(b)]. Upon drying, we observe the disappearance of the wrinkles and reappearance of the original smooth surface. This response can be cycled simply by the swelling/de-swelling process.

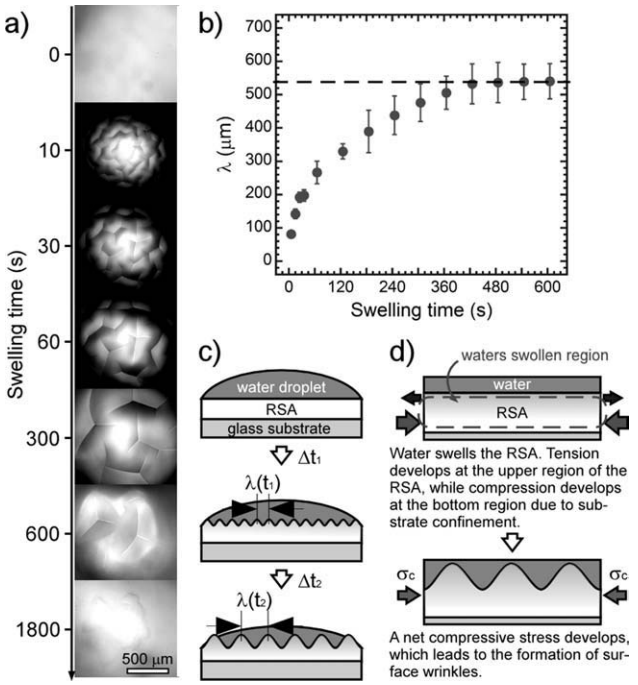

FIGURE 1 (a) Formation of surface wrinkles and their dynamic evolution with swelling time in water. (b) Increase in wavelength (λ) versus swelling time. (c) Schematic of the increase in wavelength and amplitude with swelling time. (d) Mechanism of the wrinkle formation.

Solvent-induced wrinkling has been observed in a variety of materials and is associated with the competition between osmotic pressure and lateral confinement [Fig. 1(c,d)].[7–9,13,14,16,17] Water absorption causes swelling of the free surface of the RSA. However, lateral expansion is constrained by the rigid substrate. This nonuniform swelling leads to a net compressive force developing at the free surface of the RSA and subsequent formation of surface wrinkles. Similar to other materials, the wavelength grows with swelling time and is determined by the relative thicknesses of the swollen and unswollen layers of the film.

Next, we measure the adhesion of the RSA in contact with the gelatin surface [Fig. 2(a)]. A representative force-time history of the contact adhesion test is presented in Figure 2(b). The contact area grows laterally as the RSA probe is compressed into the gelatin until the maximum compressive force is reached. At this point, the interface is allowed to dwell for a predetermined contact time. Then, the probe retracts from the gelatin surface until the entire interface separates. We use the maximum tensile force (P_s) to compare the different testing conditions [Fig. 2(c)].

Figure 2(b) shows that the RSA-gelatin interface develops surface wrinkles with a similar morphology as shown in Figure 1. This result is observed in all the materials and suggests that the RSA is wrinkling primarily due to water absorption from the gelatin. Additionally, the wrinkle morphology evolves during the testing time, which again is consistent with results in Figure 1. To understand the

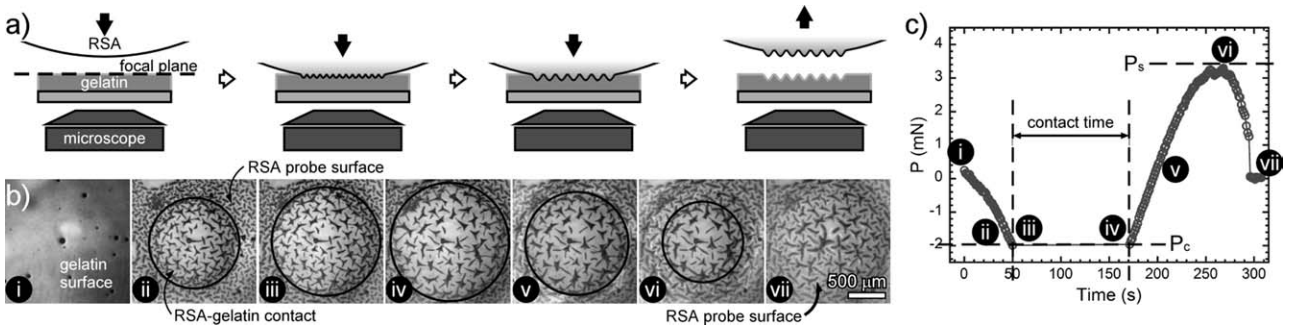

FIGURE 2 (a) Contact adhesion test for the RSA hemisphere with the gelatin surface. (b) The optical micrographs describe the interfacial contact history of a representative sample illustrating the formation and separation of a wrinkled interface. The area within the enclosed circle is the region in contact, demonstrating the formation of surface wrinkles. Outside this contact area, only the RSA lens develops surface wrinkles as evidenced by the out-of-focus surface wrinkles. (c) Force-time history of the adhesion test.

contributions of dynamic surface wrinkles to interfacial adhesion, we perform a series of adhesion tests with different contact times. We select 600 s as the longest contact time based on the time required for the surface wrinkles to stabilize as observed in Figure 1(b). Figures 3(a) summarizes P_s and $P_{s,n}$ as a function of contact time. For comparison purposes, we use the normalized separation load ($P_{s,n}$) to evaluate relative enhancement in adhesion. This normalized load is obtained by taking the ratio of P_s at time $= t$ to P_s at time $= 0$ s. When comparing the longest contact time against the shortest, we find that adhesion is enhanced by >50%. For the highest enhancement observed, we find that the separation strength, defined as the separation force normalized by the contact area, $\approx 2.7 \times 10^3$ N/m^2.

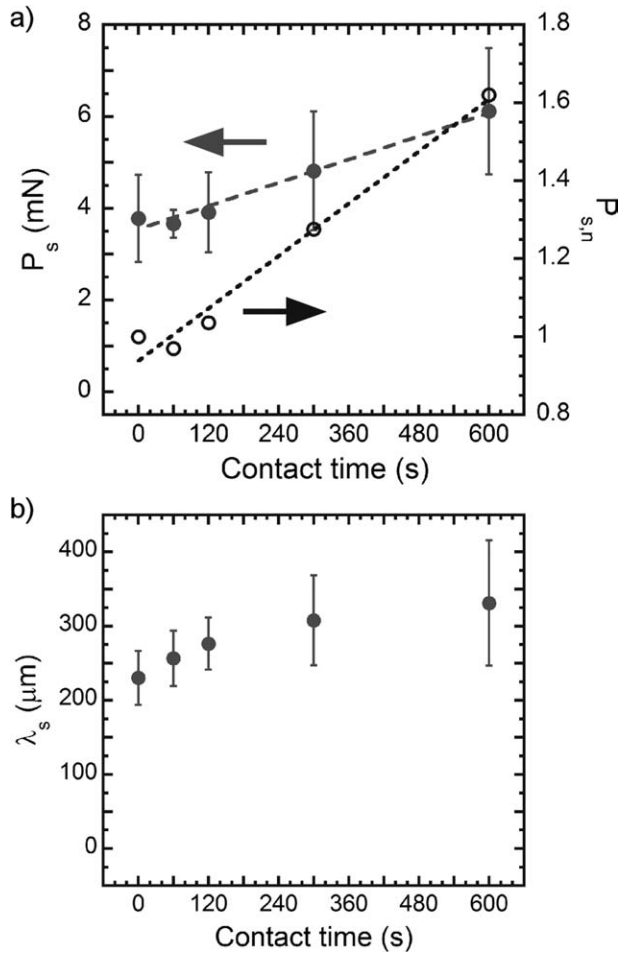

FIGURE 3 (a) P_s and $P_{s,n}$ versus contact time for the RSA-gelatin. (b) Changes in wavelength at P_s (λ_s) versus contact time.

DISCUSSION

Adhesion enhancement with contact time, or "tack", is one mechanism of interfacial control for dry pressure-sensitive adhesives (PSA). The mobile polymer chains of the PSA facilitate viscous flow, thus improving true interfacial contact with a rough surface. Similarly, we consider this chain diffusion process across the RSA-gelatin interface as a possible mechanism of enhanced adhesion. In general, the time-scale when "tack" improves is defined by the Rouse time (τ_e) of the polymer chains.[18] For typically PSAs, $\tau_e \sim 1$ s,[18] while in gelatin, $\tau_e \sim 0.01$ s.[19] These relaxation times are significantly shorter than the contact times investigated, thus suggesting that "tack" is probably not a primary mechanism of adhesion for our materials.

To identify a possible mechanism for enhancement; we consider the separation process at P_s. First, we consider a simpler separation process observed for typical PSAs. We choose crosslinked polydimethyl siloxane (pdms) as the smooth adhesive and visualize the separation process as it interacts with the gelatin surface. Here, the separation initiates at the periphery of the pdms-gelatin interface, and proceeds through a smooth and continuous crack propagation process [Fig. 4(a)]. In this case, the contact perimeter, or line (L_s), is a key geometric length-scale in defining the maximum force required for separation (P_s),

$$P_s = c \cdot (G_c L_s) \tag{1}$$

where c is a geometric constant.[20] The interesting result of this relationship is that it is independent of the elastic modulus and contact area of the interface. Based on this relationship, for an interface with a constant value of G_c, P_s can be

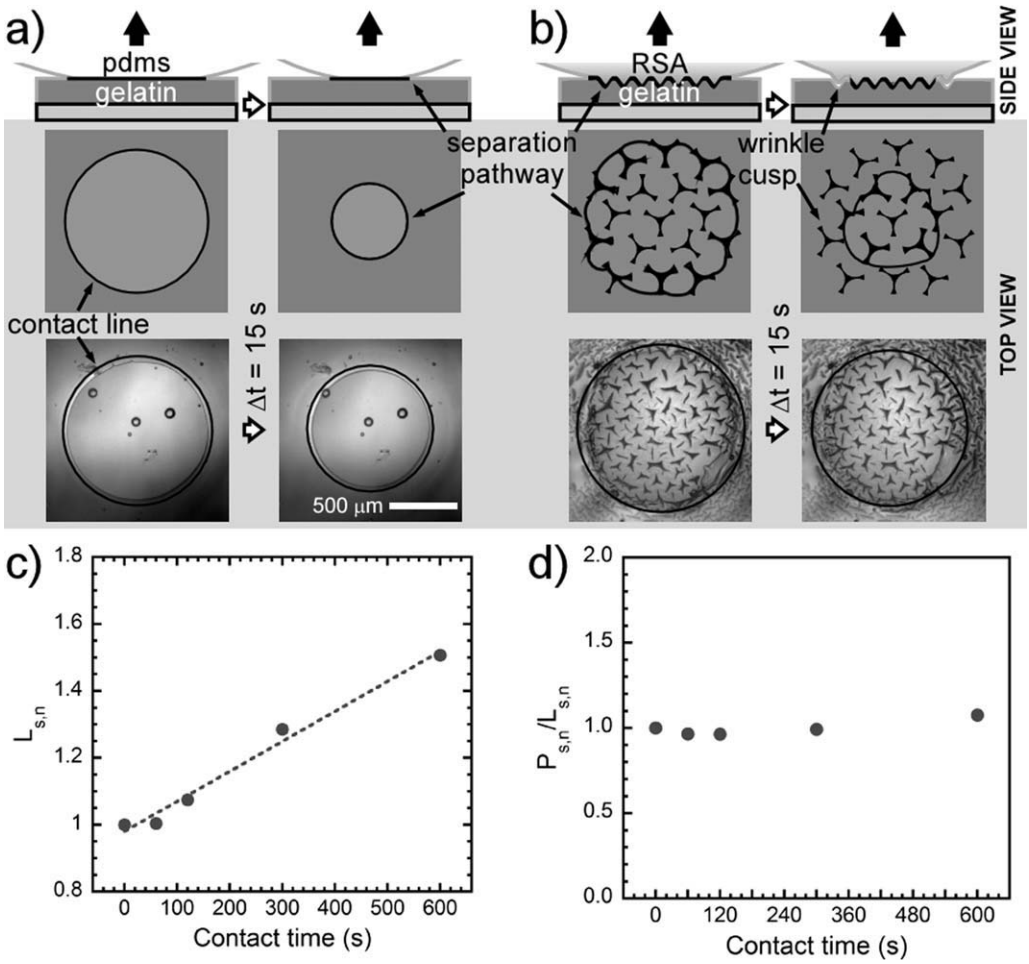

FIGURE 4 (a) Separation of the pdms-gelatin interface. (b) Separation of the RSA-gelatin interface. (c) $L_{s,n}$ versus contact time for the RSA-gelatin system at P_s. (d) Ratio of $P_{s,n}$ and $L_{s,n}$ as a function of contact time.

tuned by changing the total contact line. L_s is increased to enhance adhesion and decreased to improve release. This contact line control is a widely-utilized strategy for patterned adhesives.[3,17,21–25]

The surface wrinkles define a complex topological interface that enhances the total contact line at separation [Fig. 4(b)]. Unlike the separation process of the pdms-gelatin system characterized by the smooth crack propagation, the separation for the RSA-gelatin system occurs through a discontinuous crack initiation-propagation process. As the crack front traverses along the wrinkled interface, the wrinkled topography disrupts crack propagation by locally pinning the contact line from separating smoothly. In other words, the crack front, which is defined by the line length of the roughness, must reinitiate interfacial separation when it encounters a wrinkle. This leads to a lengthening of L_s and overall enhancement in P_s. To understand the effects of contact time with contact line, we relate the normalized contact line at separation ($L_{s,n}$) to contact time [Fig. 4(c)]. The normalized contact line is defined as the ratio of the L_s at contact time $= t$ to L_s at contact time $= 0$ s ($L_{s,n} = L_{s,t}/L_{s,t=0}$). While previous work has demonstrated that the wrinkle wavelength is the primary length-scale of control,[17] our results here suggest that both the wrinkle wavelength and amplitude contribute to the greater resistance for crack propagation by lengthening L_s, which enhances P_s. As an assessment of the relative changes in G_c with contact time, we take the ratio of $P_{s,n}$ to $L_{s,n}$ by using eq 2:

$$\frac{P_{s,n}}{L_{s,n}} \propto \frac{G_{c,t}}{G_{c,t=0}} \tag{2}$$

From Figure 4(d), we find that $P_{s,n}/L_{s,n}$ is nearly contact time independent and suggests that the adhesion energy is a constant value. While further studies are needed to understand the effects of wrinkle amplitude and wavelength on the local separation process of dynamic wrinkled surface, our results illustrate the importance of local contact geometry on the adhesion of soft materials.

CONCLUSION

This work presents an alternative approach for tailoring adhesion by strengthening interfacial contact through dynamic surface morphology. The primary advantage lies in the

application of the approach to a broad range of materials. Because it relies on improving interfacial strength through dynamic change in surface morphology, it is amenable to different materials with a variety of surface chemistries. We envision this mechanism of adhesion will inspire alternative approaches to the future development of biomedical tape-based adhesives since these materials require interfacing with hydrated, compliant materials such as soft tissues.

ACKNOWLEDGMENTS

The authors thank Christopher M. Stafford at NIST Polymers Division for the use of the contact adhesion test instrument. EPC would like to thank Alfred J. Crosby for helpful suggestions. Funding is provided by the NSF NIRT grant 0609182 and NIH grant DE013023 to RL, CIMIT through the U.S. Army grant W81XWH-07-2-0011 and NIH GM086433 to JMK. This work was also supported in part by the Commonwealth of Massachusetts through the Technology Transfer Center at the University of Massachusetts to JMK. American Heart Association Grant 0835601D to JMK.

REFERENCES AND NOTES

1 Jeong, B.; Gutowska, A. *Trends Biotechnol.* **2002**, *20*, 305–311.

2 Reddy, S.; Arzt, E.; del Campo, A. *Adv. Mater.* **2007**, *19*, 3833–3837.

3 Lin, P.; Vajpayee, S.; Jagota, A.; Hui, C.-H.; Yang, S. *Soft Matter* **2008**, *4*, 1830–1835.

4 Chang, D. P.; Dolbow, J. E.; Zauscher, S. *Langmuir* **2007**, *23*, 250–257.

5 Sun, T.; Wang, G.; Feng, L.; Liu, B.; Ma, Y.; Jiang, L.; Zhu, D. *Angew. Chem. Int. Ed.* **2004**, *43*, 357–360.

6 Lin, P.; Yang, S. *Soft Matter* **2009**, *5*, 1011–1018.

7 Kim, J.; Yoon, J.; Hayward, R. C. *Nat. Mater.* **2010**, *9*, 159–164.

8 Southern, E.; Thomas, A. G. *J. Polym. Sci., Part. A: Polym. Chem.* **1965**, *3*, 641–646.

9 Tanaka, T.; Sun, S.-T.; Hirokawa, Y.; Katayama, S.; Kucera, J.; Hirose, Y.; Amiya, T. *Nature* **1987**, *325*, 796–798.

10 Bowden, N.; Brittain, S.; Evans, A. G.; Hutchinson, J. W.; Whitesides, G. W. *Nature* **1998**, *393*, 146–149.

11 Hayward, R. C.; Chmelka, B. F.; Kramer, E. J. *Macromolecules* **2005**, *38*, 7768–7783.

12 Chan, E. P.; Crosby, A. J. *Soft Matter* **2006**, *2*, 324–328.

13 Trujillo, V.; Kim, J.; Hayward, R. C. *Soft Matter* **2008**, *4*, 564–569.

14 Guvendiren, M.; Yang, S.; Burdick, J. A. *Adv. Funct. Mater.* **2009**, *19*, 3038–3045.

15 Sidorenko, A.; Krupenkin, T.; Taylor, A.; Fratzl, P.; Aizenberg, J. *Science* **2007**, *315*, 487–490.

16 Guvendiren, M.; Burdick, J. A.; Yang, S. *Soft Matter*, in press.

17 Chan, E. P.; Smith, E. J.; Hayward, R. C.; Crosby, A. J. *Adv. Mater.* **2007**, *20*, 711–716.

18 Creton, C.; Leibler, L. *J. Phys. B: Polym. Phys.* **1996**, *34*, 545–554.

19 Sharma, J.; Bohidar, H. B. *Colloid Polym. Sci.* **2000**, *278*, 15–21.

20 Varenberg, M.; Peressadko, A.; Gorb, S.; Arzt, E. *Appl. Phys. Lett.* **2006**, *89*, 121905.

21 Geim, A. K.; Dubonos, S. V.; Grigorieva, I. V.; Novoselov, K. S.; Zhukov, A. A.; Shapoval, S. Y. *Nat. Mater.* **2003**, *2*, 461–463.

22 Spolenak, R.; Gorb, S.; Gao, H.; Arzt, E. *Proc. R. Soc. A* **2004**, *461*, 305–319.

23 Thomas, T.; Crosby, A. J. *J. Adhes.* **2006**, *82*, 311–329.

24 Chan, E. P.; Greiner, C.; Arzt, E.; Crosby, A. J. *MRS Bull.* **2007**, *32*, 496–503.

25 Chan, E. P.; Ahn, D.; Crosby, A. J. *J. Adhes.* **2007**, *83*, 473–489.